

## Apatite internal structure and estimation of initial fluorine concentration in the Western Carpathians granitoids

ALEXANDRE AUBIN<sup>1\*</sup>, IGOR BROSKA<sup>1</sup>, MICHAL KUBIŠ<sup>1</sup> and JAROMÍR LEICHMANN<sup>2</sup>

<sup>1</sup>Geological Institute of the Slovak Academy of Science, Dúbravská cesta 9, 840 05 Bratislava, Slovak Republic.  
E-mail: [geolbros@savba.sk](mailto:geolbros@savba.sk)

<sup>2</sup>Institute of Geology and Palaeontology, the Masaryk University, Kotlářská 2, 611 37 Brno, Czech Republic

\*Current address: Department of Earth Sciences, Biological & Geological Building, The University of Western Ontario, London, Ontario, Canada N6A 5B7. E-mail: [aubin2@uwo.ca](mailto:aubin2@uwo.ca)

**Abstract.** A study of primary apatite (white and dark pigmented) in Western Carpathians granitoids revealed three types of internal structure: oscillatory zoning, presence of old core (inheritance or two generation origin), and absence of internal structure. Secondary apatite is typically found in the specialized S-type granitoids, forming minute grains within plagioclase as a result of P leaching from the berlinite molecule in the alkali feldspars. The formation of tiny apatite veinlets and apatite-bearing veins in the host rocks is possible considering the high mobility of P. Apatite composition depends both on the geotectonic origin of the host rock and on granitoid evolution. Mn and Fe contents in apatite are indicators of the geotectonic setting of the granitoids; low Mn and Fe content being characteristic of I-type granitoids, as opposed S-type or A-type, which both show a higher Fe content. Apatite composition has been used for the estimation of primary F content in the felsic melts. Fluorine content is approximately 10 times lower in the volatile phases than in the melt. S-type and I-type granitoids show similar fluorine concentration in the liquidus (60–90 ppm). A significantly higher primary F content in the Western Carpathian granitoid melts was calculated in the specialized S-type granitoids (cca 300 ppm) and A-type granitoids (cca 1 000 ppm). This shows that apatite composition in granitoids can be used both for determining the geotectonic setting and the initial F content of the felsic melts.

**Key words:** apatite, black apatite, fluorine, S-type granites, I-type granites, A-type granites.

### Introduction

Apatite is considered an abundant accessory mineral in the more basic granitoids of the Western Carpathians and less common in the assemblages with monazite (e.g. Hovorka & Hvožd'ara, 1965; Hovorka, 1968; Veselský & Gbelský, 1978; Chovan & Határ, 1978). The most important information derived from apatite in the Western Carpathians was from fission track dating of the various granitoid types, which determined uplift rates in the Tatric and Veporic units (Kráľ, 1977; Danišík et al., 2004). Apatite has also been used in establishing the compositional criteria for the distinction of the S-, I- and A-type granitoids (Broska et al., 2004). Carboniferous impurities in the apatite, such as graphite, carbides and hydrocarbons, recognized in some Tribeč and Malá Fatra Mts. granitoids were interpreted as the results of assimilation of black shales during granitoid emplacement in a reducing regime (Broska et al., 1992).

Despite the fact that apatite is one of the most common accessory phases in the granitoid rocks of the Western Carpathians (e.g. Hovorka & Hvožd'ara, 1965; Hvožd'ara & Határ, 1978), many questions remain concerning its structure and composition. The objectives of this study were to 1) determine the internal structure of apatite using cathodoluminescence techniques, 2) outline the significance of apatite composition with respect to the host rock, and 3) use apatite for modelling of the fluorine

concentration in the initial silicic melts; the latter becoming more frequently used as a method derived from apatite analysis (e.g. Sallet, 2000; Mathez & Webster, 2005).

### Sample location

Apatite grains were derived from various S-, I- and A-type granitoids from the Tatric, Veporic, and Gemeric units of the Western Carpathians (Fig. 1). The S-type granitoids are typically of Lower Carboniferous age, whereas I-type granitoids are of Upper Carboniferous age (Petrík et al., 1994; Petrík & Broska, 1994; Petrík & Kohút, 1997). The rift-related, A-type granitoids are Permian in age and are located in the Gemeric unit, along with the Permo-Triassic specialized S-type granitoids (Uher & Broska, 1996; Broska & Uher, 2001). In addition to the ZK set samples (Macek et al., 1982), granitoid specimens from the Tribeč, Žiar, Malá Fatra, Vysoké Tatry Mts., Hnilec a Dlhá dolina localities in Slovenské Rudohorie were chosen because of the large amount of apatite analyses available (Broska et al. 2004). The distribution of dusky apatite in the samples is presented in Table 1, in addition to abundances of monazite and allanite.

### Methods

The granitoid samples were crushed and heavy minerals were extracted using a Wilfley table and bromoform

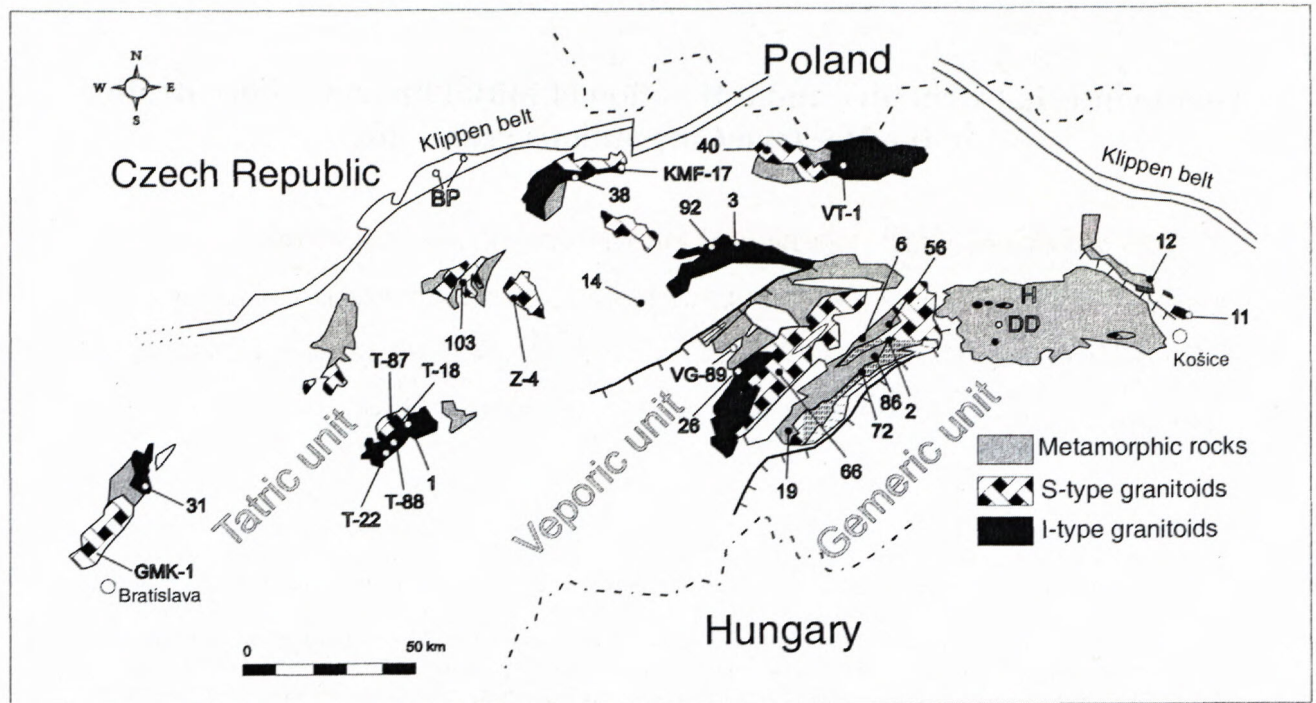


Figure 1. Location of the samples studied in this paper. The samples with only numbers are part of the ZK-series. The ZK-prefixes have been dropped for space reasons. Only the granitoids are shown. The locations of the samples are taken from Macek et al. (1982). The position of samples in the Gemeric unit: H – Hnilec granite; DD – Dlhá dolina valley with the hidden granites.

(S.G. 2.85). Minerals were then separated according to their magnetic properties using a Cook magnetic separator. The apatite grains were hand-picked using a binocular microscope, and were mounted in epoxy on thin sections. The thin sections were then polished to expose the middle of the apatite grains.

Cathodoluminescence microscopy (CL) was conducted using a Simon Neuser HC/LM2 hot cathode CL microscope at Masaryk University in Brno (Czech Republic). Analytical conditions were at 14 kV accelerating voltage, and 10 mA/mm<sup>2</sup> current density. The films used for CL photography were Fujichrome MS 100/1000, exposed and developed at 800 ASA. The time of exposure varied from 20 to 100 seconds.

Microprobe analyses were done on 1) a JEOL JXA-733 Superprobe (Geological Survey of Slovak Republic) using fluorapatite as a standard and 2) a Cameca SX50 electron microprobe at the National History Museum, London. During measurement, the operating conditions were 15kV, with a 25 nA beam current and a beam diameter of 1-5 µm. Care was taken in determining of F, and a PC1 (multi-layer crystal) was used to eliminate potential interference from the P 3<sup>rd</sup>-order line.

Carbon analyses on sample T-87 were performed on a STROHLEIN C-MAT 5500 infrared organic carbon detection instrument (Geological Institute of the Slovak Academy of Sciences). The specimens were burned in an oxygen current with a gradual increase of temperature from 70 °C to 1000 °C. The bulk carbon content of the sample was measured, all inorganic carbon was removed by HCl, and the remaining carbon (organic) was measured and compared with the calibration standard.

## Results

### Apatite distribution

Early magmatic differentiates of I-type granitoid suites in the Western Carpathians are the most rich in apatite because they often contain several hundred g/t and locally more than 1000 g/t. The amount of apatite decreases in differentiated I-type granitoids, which is reflected by the decrease of P concentration in these rocks. Apatite often forms stubby, milky or yellow pigmented crystals which are usually located within biotite and in interstices between grains. S-type granitoid suites, which are relatively poor in apatite, contain crystals that are smaller. The concentration of black pigmented apatite (dusky apatite) is locally common in S-type granitoids but dusky apatite is also present in some I-type granitoids (Table 1).

### Apatite composition

According to primary magmatic apatite composition, the essential known criteria for the recognition of the I-, S- and A-type granitoids is the concentration of Mn and Fe along with REE distribution. The Mn content of apatite in the Western Carpathians increases with the peraluminosity of granitoids and with decreasing  $fO_2$ . Thus, apatite from S-type granitoids has slightly higher Mn contents in comparison to apatite from the I-type granitoids. Apatite in the A-type granitoids is enriched in Fe and HREE similar to apatite from specialized tin-bearing S-type granitoids, which show an increase in Y

and HREE content (Broska et al., 2004). General Mn and Fe distribution within the granitoid suites is shown in Fig. 2.

Table 1: Characteristics of the samples used in this paper in regard to their allanite, monazite and black apatite contents. The position of the samples is given in Figure 1. The ZK-series is represented here without the ZK-prefix.

Sample #	Granitoid type	Monazite (g/ton)	Allanite (g/ton)	% of black apatite in total apatite
KMF-17	S	30	0	85
T-18	S	200	15	80
T-22	I	0	90	0
T-36	I	0	140	0
T-87	S	60	0,5	99
VT-1	I	n.d.	n.d.	0
Z-4	S	n.d.	n.d.	15
ZK-1	I	1	470	Tr
ZK-2	S	6	0,5	3
ZK-3	S	16	5	Tr
ZK-6	I	0,5	30	2
ZK-9	I	0,5	38	1
ZK-11	S	33	48	6
ZK-12	I	0	958	50
ZK-14	S	19	0	1
ZK-19	S	33	0	3
ZK-26	S	0	0	Tr
ZK-31	I	0	12	80
ZK-38	I	0	348	10
ZK-40	S	42	3	50
ZK-56	S	1	0	2
ZK-66	I	n.d.	n.d.	Tr
ZK-72	S	12	0,5	40
ZK-86	I	6	292	2
ZK-92	S	18	7	Tr
ZK-103	S	4	0	2

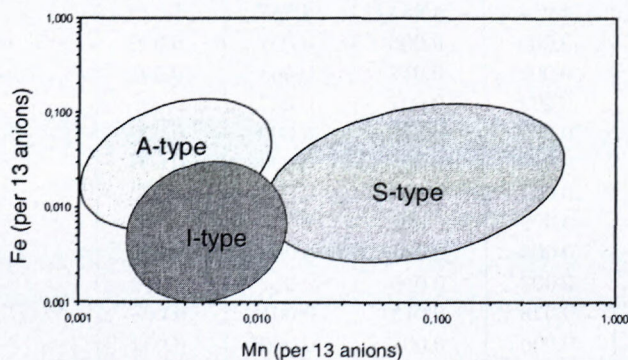


Figure 2: General scheme of Mn and Fe distribution in the granitoids of the Western Carpathians. (Generalized according to Broska et al. 2004).

In addition to minor feric and REE components, volatiles phases are also an important discriminative component of apatite. Although the concentrations of F and Cl are similar in all granitoid, there are slight differences in the distribution that help differentiate between the different types. Table 2 presents the results of mi-

croprobe analysis of characteristic apatite grains from all principal granitoid suites in the Western Carpathians. The mean concentration of fluorine is generally above 3 wt % and chlorine is often beyond the detection limit in the A-type granitoids, but is quite high in the I-type suites (Fig. 3). All analyzed apatites are fluorapatites (Fap). The highest concentration of fluorapatite and hydroxylapatite molecule is present in the specialized S-type granitoids (Fig. 3). The lower Cl concentration in apatite from the S-type granitoids in comparison to I-type granitoids was explained by Sha & Chappel (1999) as a selective loss of Cl in the sedimentary protolith, because of higher Cl solubility in aqueous solutions.

### Internal structure

Apatite grains under the binocular (B), polarised (M), cathodoluminescence (CL), and back-scattered electron (BSE) microscopes contain three types of internal structures: oscillatory zoning, relict cores (or two generation origin), and absence of internal structure.

*Oscillatory zoning* (Fig. 4A): This pattern is observed mainly in I-, less in S-type samples, in white and dark pigmented apatite. It consists of small dark and light zones (in CL) that are repeated from the core to the rim of the grains. The thickness of the zones can vary from smaller than a micron to tens of microns. Typical grains are composed of a central zone (core), which is generally black. Oscillatory zoning was also observed on the polarised microscope in the dark pigmented apatite, but was invisible in the white apatite. The zones that are darker in CL appear brighter on BSE images.

Two types of mechanisms have been suggested for the origin of oscillatory zoning (Shore & Fowler, 1996): extrinsic mechanisms and intrinsic mechanisms. The extrinsic mechanisms refer to changes outside the grains (mixing of magma, changes in composition of volatile phases, etc.) whereas intrinsic mechanisms refer to changes that occur within the crystal during the crystallisation process (diffusion of elements, small scale convection currents, adsorption of minor and trace elements). It is believed that the internal structure of the studied apatite from the Western Carpathians is a result of crystal growth under certain conditions and that the rapidity of growth produced the oscillatory zoning.

The difference in colour contrast in CL zoning (Fig. 4B) is probably due to the variation of Mn and REE concentrations, elements which are known to be the main activators in apatite under CL (Murray & Oreskes, 1997). It is believed that the oscillatory zoning in apatite is caused by the variation of the concentration and/or nature of Mn and REEs during magma crystallization (intrinsic mechanism). Cherniak (2000) proved that REE zoning occurs in fluorapatite.

*Old cores* (Fig. 4C,D): In some samples, the presence of an old (inherited) core was visible under CL but not in BSE images. Both white and dark pigmented grains contain inherited cores, and they generally occur in S-type granitoids. The old cores are present as rounded inclu-

Table 2: Representative analyses of apatites from the S-, I-, A- and spec. S-type granitoids. The concentration of the elements and oxides are in wt %.  $X_{FAP}^{Ap}$  represents the mole fraction of fluorine in apatite,  $X_{ClAp}^{Ap}$  represents the mole fraction of chlorine in apatite and  $X_{HAp}^{Ap}$  represents the mole fraction of hydrogen in apatite. Sample GK-8 P represents primary apatite and GK-8 S is secondary one (minute grain in alkaline feldspar).

Sample	Z-4 S-type	GMK-1 S-type	T-88 I- type	ZK-38 I-type	VG-89 A-type	BP-20 A-type	GK-8 P sS-type	GK-8 S sS-type
SO <sub>3</sub>	0.00	0.00	0.25	0.05	0.02	0.02	0.00	0.04
P <sub>2</sub> O <sub>5</sub>	42.18	41.96	41.80	43.14	39.60	39.78	41.72	42.00
SiO <sub>2</sub>	0.22	0.06	0.16	0.04	0.35	0.40	0.05	0.05
CaO	54.13	54.20	55.76	54.93	52.29	53.18	52.65	56.07
La <sub>2</sub> O <sub>3</sub>	0.05	0.00	0.07	0.00	0.00	0.19	0.04	0.00
Ce <sub>2</sub> O <sub>3</sub>	0.16	0.08	0.11	0.10	0.18	0.53	0.11	0.11
Pr <sub>2</sub> O <sub>3</sub>	0.00	0.00	0.00	0.04	0.10	0.23	0.07	0.05
Nd <sub>2</sub> O <sub>3</sub>	0.00	0.00	0.03	0.06	0.26	0.38	0.00	0.00
Sm <sub>2</sub> O <sub>3</sub>	0.00	0.00	0.00	0.00	0.00	0.15	0.00	0.01
Gd <sub>2</sub> O <sub>3</sub>	0.00	0.00	0.00	0.00	0.06	0.13	0.03	0.00
Er <sub>2</sub> O <sub>3</sub>	0.00	0.00	0.00	0.03	0.15	0.06	n. a.	n. a.
Dy <sub>2</sub> O <sub>3</sub>	0.00	0.00	0.00	0.06	0.15	0.05	0.26	0.02
Yb <sub>2</sub> O <sub>3</sub>	0.00	0.00	0.00	0.00	0.08	0.00	0.05	0.00
Y <sub>2</sub> O <sub>3</sub>	0.10	0.11	0.12	0.26	0.60	0.32	0.02	0.07
PbO	0.00	0.00	0.00	0.00	0.00	0.02	0.00	0.07
ThO <sub>2</sub>	0.06	0.04	0.05	0.01	0.02	0.04	0.01	0.00
UO <sub>2</sub>	0.07	0.05	0.03	0.00	0.00	0.00	0.10	0.02
Al <sub>2</sub> O <sub>3</sub>	0.01	0.00	0.00	0.05	0.00	0.02	0.00	0.03
+FeO	0.20	0.33	0.12	0.04	0.70	0.96	0.59	0.09
MnO	0.19	0.30	0.10	0.02	0.59	0.12	3.04	0.27
MgO	0.02	0.00	0.00	0.01	0.00	0.01	0.00	0.00
Na <sub>2</sub> O	0.13	0.12	0.08	0.05	0.13	0.06	0.05	0.07
SrO	0.06	0.06	0.08	0.12	0.00	0.00	0.04	0.21
F	2.53	3.10	2.50	2.22	3.49	2.80	3.72	3.41
Cl	0.04	0.00	0.05	0.02	0.02	0.00	0.12	0.02
OH	0.49	0.26	0.51	0.64	0.04	0.34	-0.01	0.15
total	101.20	100.67	101.82	101.88	99.38	99.79	102.67	102.76
O=F.Cl	1.07	1.30	1.06	0.94	1.47	1.18	1.59	1.44
TOTAL	100.13	99.36	100.76	100.94	97.91	98.61	101.08	101.32
S	0.000	0.000	0.020	0.004	0.002	0.002	0.000	0.003
P	3.045	3.025	2.992	3.073	2.941	2.945	2.978	2.977
Si	0.019	0.005	0.014	0.003	0.030	0.035	0.004	0.004
Ca	4.945	4.944	5.051	4.952	4.914	4.983	4.757	5.029
La	0.001	0.000	0.002	0.000	0.000	0.006	0.001	0.000
Ce	0.005	0.002	0.003	0.003	0.006	0.017	0.003	0.003
Pr	0.000	0.000	0.000	0.001	0.003	0.007	0.002	0.002
Nd	0.000	0.000	0.001	0.002	0.008	0.012	0.000	0.000
Sm	0.000	0.000	0.000	0.000	0.000	0.005	0.000	0.000
Gd	0.000	0.000	0.000	0.000	0.002	0.004	0.001	0.000
Er	0.000	0.000	0.000	0.000	0.002	0.004	n. a.	n. a.
Dy	0.000	0.000	0.000	0.002	0.004	0.001	0.007	0.000
Yb	0.000	0.000	0.000	0.000	0.002	0.000	0.001	0.000
Y	0.005	0.005	0.005	0.012	0.028	0.015	0.001	0.003
Pb	0.000	0.000	0.000	0.000	0.000	0.001	0.000	0.002
Th	0.001	0.001	0.001	0.000	0.000	0.001	0.000	0.000
U	0.001	0.001	0.001	0.000	0.000	0.000	0.002	0.000
Al	0.001	0.000	0.000	0.005	0.000	0.002	0.000	0.003
Fe	0.014	0.024	0.009	0.003	0.051	0.070	0.042	0.006
Mn	0.014	0.021	0.007	0.001	0.044	0.009	0.217	0.019
Mg	0.003	0.000	0.000	0.001	0.000	0.001	0.000	0.000
Na	0.021	0.020	0.014	0.008	0.021	0.011	0.008	0.011
Sr	0.003	0.003	0.004	0.006	0.000	0.000	0.002	0.010
XApFAP	0.68	0.83	0.67	0.59	0.97	0.78	0.99	0.90
XApClAp	0.01	0.00	0.01	0.00	0.00	0.00	0.01	0.00
XApHAp	0.31	0.17	0.33	0.41	0.03	0.22	0.00	0.10

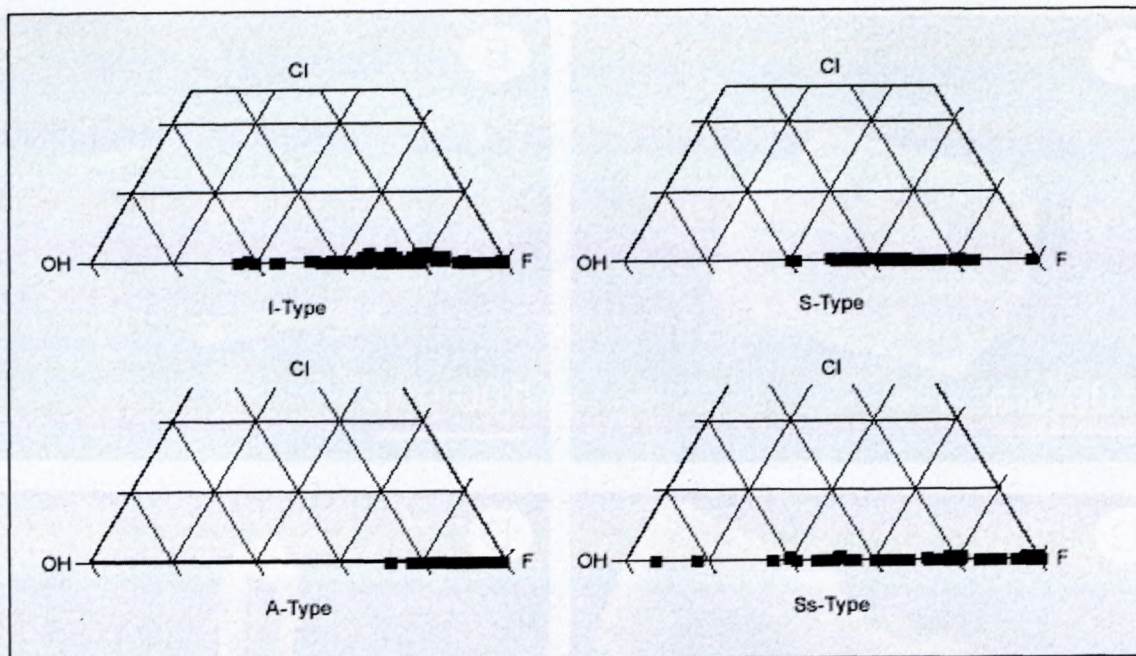


Figure 3: Ternary diagram of apatite composition in respect to granitoid types. F: fluorapatite; Cl: chlorapatite; OH: hydroxylapatite. The Cl axis is cut at 50%. The apatites from I-type granitoids tend to have a generally higher Cl component whereas the apatites from A-type granitoids are generally above 80% fluorapatite. Differences between the other granitoid types (S and Ss) are not as clear.

sions in the centres of the grains. They have no typical crystalline shape and are a different colour than the rest of the grain in CL (brighter and darker). The estimated volume occupied by the old cores varies from 15 vol. % to 40 vol. % of the grains.

The presence of old cores is probably due to the incorporation of partly-dissolved apatite grains into a phosphorus-saturated melt. This phenomenon occurs with the arrival of newly melted material into the magma chamber. The new melt, which is already saturated in P prevents further dissolution of the apatite and allows for the old apatite grain to act as a nucleation site for the crystallisation of new material. Harrison & Watson (1984) also mentioned that the dissolution of apatite is very fast (e.g. hundreds of years for a 500 micron grain) for melts with an average water content of 3 %, so that the only way to keep this mineral from dissolving is to saturate the melt. Therefore, it is assumed that the core is derived from a different origin than the rest of the grain. The cores carry information about protoliths, and indicate the presence of recycled crustal material (see Kohút, 1998; Petřík, 2000). The presence of old cores also indicates a lower crystallization temperature for S-type granitoids in comparison to I-type granitoids in which older cores were not observed. The same inherited core and zoning phenomenon has been observed by other authors (Dempster et al., 2003) who also suggest a dissolution-crystallization system.

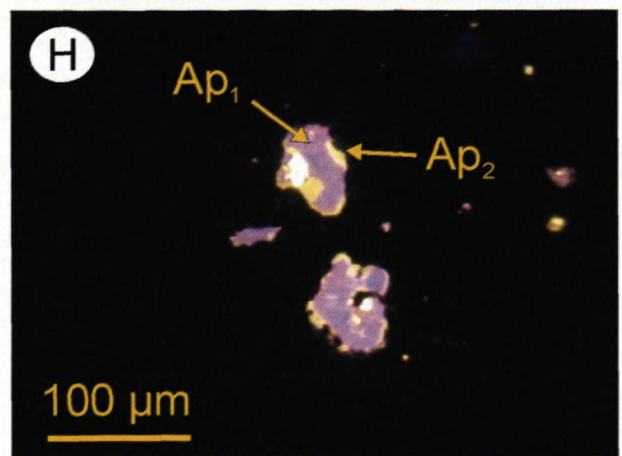
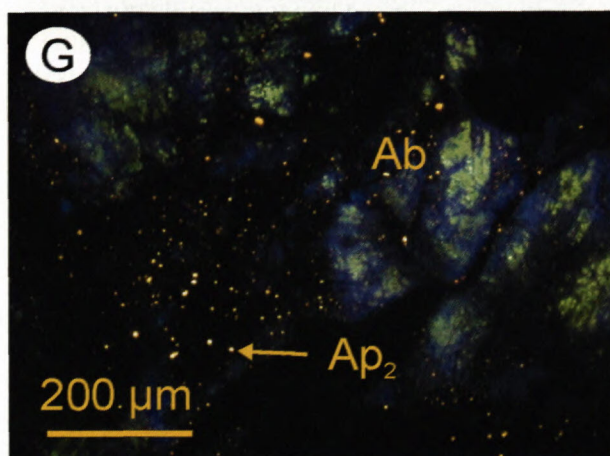
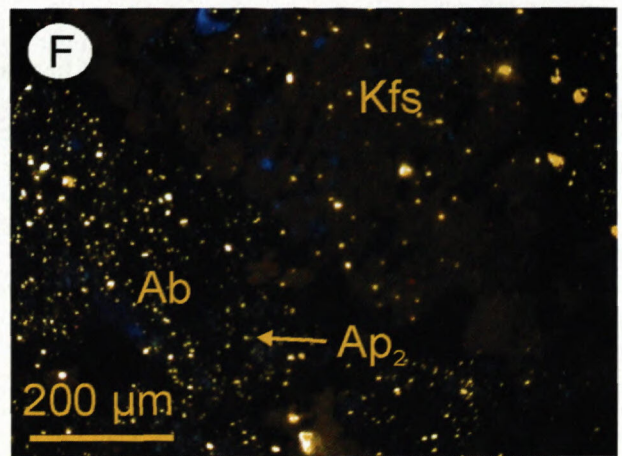
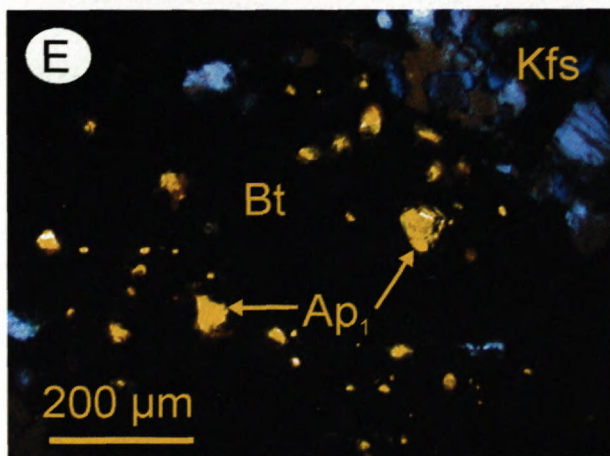
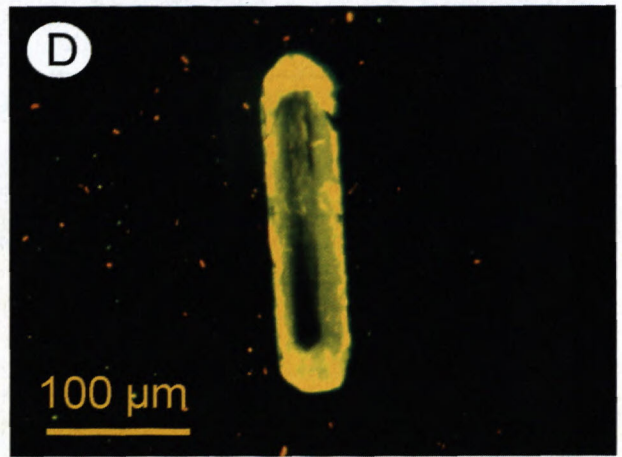
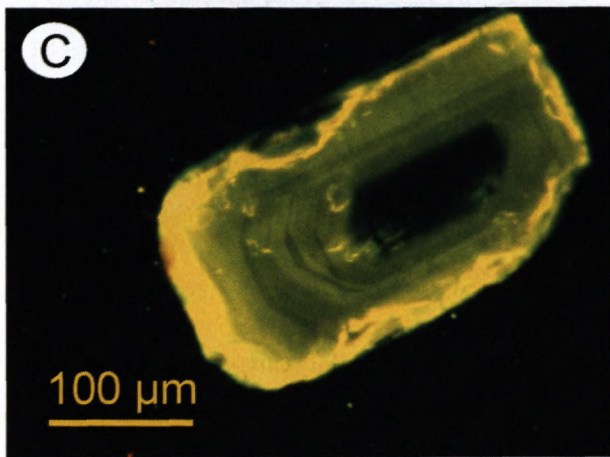
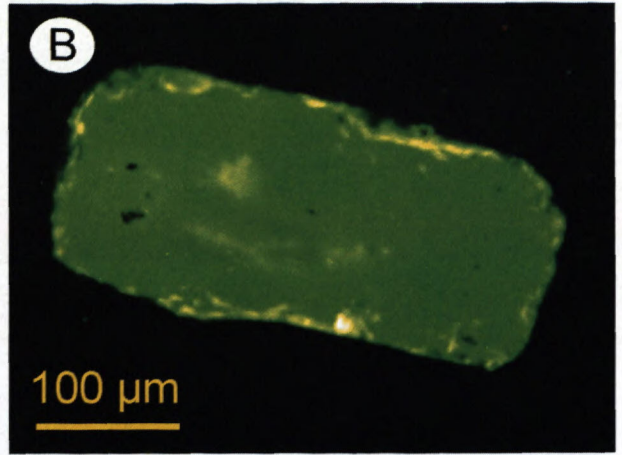
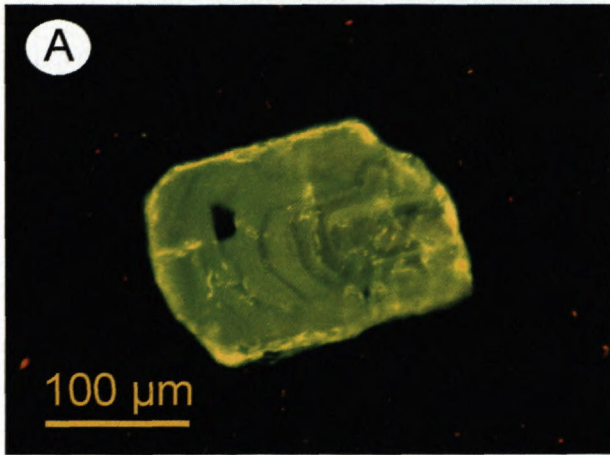
**Absence of internal structure:** Most of the studied grains (especially from I-type granitoids) have no internal structure. The images obtained from CL and BSE show uniform grains without any change in structure, which indicates rapid crystallization, probably in the early magmatic stage. Most of the studied grains con-

tained inclusions (mainly zircon, with minor biotite and albite), which were observed in all three types of internal structures.

#### Dark pigmented apatite

Two different types of dark pigmented apatite were observed, 1) dark cores inside clear apatite grains (the dark portion constitutes 100 % of the grain in some cases, but is generally around 50 %) and 2) two coexisting cores (a black inner core and a dark outer core) (Fig. 4C,D). The two types of dark pigmented apatite were observed mainly in S-type granitoids, but some were also present in I-type granitoids. When studied under CL and BSE, almost all the dark pigmented apatite presented oscillatory zoning. Under cross polarised light, the dark pigmented apatite shows a strong pleochroism, similar to that of tourmaline.

Apatite with a black inner core shows a change of crystal shape in addition to oscillatory zoning. The black core appears to be of a different crystal system (monoclinic?) and the entire grain tends to evolve towards the hexagonal shape of the apatite during its growth. Some analyses were conducted to investigate this phenomenon (carbon detection, microprobe and X-rays) and the results pointed mostly to apatite, but with another unknown phase. Murray & Oreskes (1997) mentioned that differences in CL colours (zoning for instance) could also be due to crystallographic effects. This theory could be appropriate because the shape of some dark pigmented apatite cores appears to be monoclinic. Fleet et al. (2000) experimentally proved that the substitution of REE for Ca interferes with the crystalline



system of apatite and that a transition from hexagonal system (P6<sub>3</sub>/m) to monoclinic system (P2<sub>1</sub>/b) is one of the results of this substitution.

Little or no carbon (below the detection level of the device) was found in the black pigmented apatite mentioned by Broska et al. (1992) and there were no measured foreign phases (unlike e.g. Gottesmann & Wirth, 1997). It is proposed that the variation in colour is more likely due to the presence of another mineral phase and/or to the presence of a different crystalline system (monoclinic) than the hexagonal system. The graphite extracted from the dusky apatite found by Broska et al. (1992) does not appear to be the principal factor of apatite coloration.

**Secondary apatite**

Secondary apatite is a leaching product of the berlinite molecule from the alkali feldspar (Fig. 4E,F,G,H). Berlinite, AlPO<sub>4</sub>, is isostructural with quartz or the Si<sub>2</sub>O<sub>4</sub> framework component of feldspars and is incorporated into feldspars by the coupled substitution of Al<sup>3+</sup> + P<sup>5+</sup> for 2 Si<sup>4+</sup>. This exchange is well-known as the berlinite substitution (London, 1992; 1998). Postmagmatic fluid activity releases P from feldspars or from the berlinite molecule along with Ca from the anorthite molecule, and secondary apatite can precipitate. Secondary apatite is represented by minute crystals usually within albite, but sometimes also within K-feldspar. The mass balance calculation shows that the significant amount of secondary apatite in the presented albite on Fig. 4 E,F was derived from albite with An concentration below An<sub>20</sub>. Minute apatite is often close to stoichiometric composition (Broska et al., 2002). Locally, apatite also forms small veinlets as well as veins outside of the main granitoid body (Fig. 5).

**Fluorine content**

The apatites were used to determine the amount of fluorine in the melt using the following equations (Piccoli & Candela, 1994):

$$C_F^{aq} = \frac{X_{FAp}^{Ap}}{X_{HAp}^{Ap}} \cdot \frac{1.90 \times 10^7}{18} \cdot \frac{1}{10^{\left[ \frac{0.18219 + \frac{5301.1}{T} - \frac{0.00360(P-1)}{T}}{T} \right]}}$$

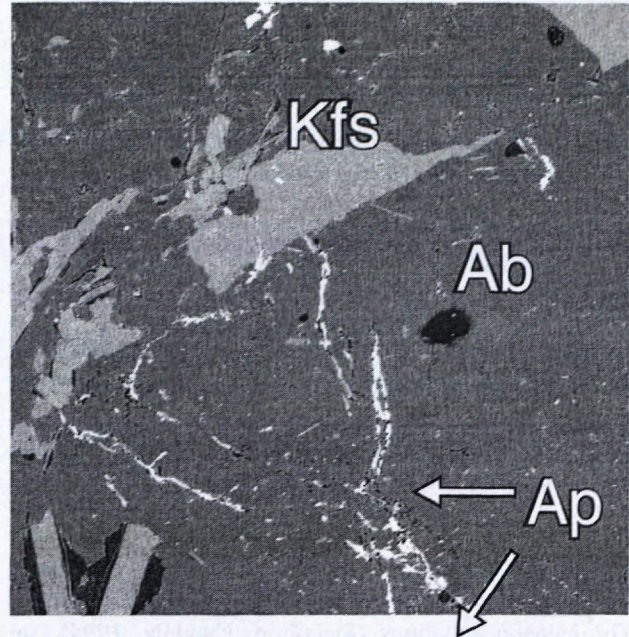


Figure 5. BSE of the apatite veinlets from the apogranite of the Dlhá dolina valley (borehole DD-20; 266 m depth). All white parts on the image represent the apatite exsolution and mobilization within alkali feldspar. (magnification 160x).

and

$$C_F^l = \frac{X_{FAp}^{Ap} \cdot 1.90 \times 10^7}{X_{HAp}^{Ap} \cdot 18} \cdot \frac{1}{10^{\left[ \frac{0.18219 + \frac{5301.1}{T} - \frac{0.00360(P-1)}{T}}{T} \right]}}$$

and

$$D_F^{aq/l} = -0.56 + 0.00093 \cdot T(^{\circ}C)$$

where the terms used are:

- $X_i^{\phi}$  mole fraction of phase component i in phase  $\phi$
- $C_i^l$  concentration of i in melt
- $C_i^{aq}$  concentration of i in magmatic volatile phase
- $D_i^{aq/l}$  partition coefficient of i between the magmatic volatile phase and melt
- $T$  temperature in Kelvin, unless specified
- $P$  pressure in bars

Figure 4: Cathodoluminescence images of primary and secondary apatite from Western Carpathian granitoids (apatite creates yellow luminescence). A: white apatite grain from sample T-22 (I-type granitoid). Oscillatory zoning is present but no core is visible. B: white apatite grain from sample ZK-40 (S-type granitoid). Note the absence of internal structure. C: dark-pigmented apatite grain from sample ZK-66 (I-type granitoid). D: dark-pigmented apatite from sample T-87 (S-type granitoid). Note the very dark core and the oscillatory zoning. E: primary apatite grains (Ap<sub>1</sub>) as inclusions in biotite (Bt). From sample GK-6, specialized S-type granitoid, Betliar area. F: secondary apatite grains (Ap<sub>2</sub>) in albite (Ab). From sample GZ-1, specialized S-type granitoid, Hnilec area. G: secondary apatite grains (Ap<sub>2</sub>) in albite (Ab). From sample GZ-1, specialized S-type granitoid, Hnilec area. H: Two generations of apatite in sample GZ-1 (specialized S-type granitoid, Hnilec area). The older generation shown in purple (violet Ap<sub>1</sub>) and the younger generation is represented in yellow (Ap<sub>2</sub>). The difference in apatite luminescence colour is due to the different compositions of the two generations: purple being generally activated by trace quantities of rare earth element ions (Ce<sup>3+</sup>, Eu<sup>2+</sup>, Sm<sup>3+</sup>, Dy<sup>3+</sup> and Nd<sup>3+</sup>), whereas yellow is generally activated by Mn<sup>2+</sup> (Marshall, 1988).

The temperature used for the calculation was the AST (apatite saturation temperature) (Harrison & Watson, 1984) as suggested by Piccoli & Candela (1994), although this is quite unrealistically high. All samples were calculated on the basis of a 300 MPa pressure.

The results, which are presented in Table 3, show a clear difference in fluorine concentrations (in the melt and in the volatile phase) among the different kinds of granitoid rocks (I-, S- and A-type). Fluorine content in the volatile phase is about 10 times lower than in the melt. The amount of fluorine in the S-type melt is similar to samples with I-type affinity except for the specialized S-type granitoids of the Gemeric unit in which a high primary amount of F exists (Kubiš and Broska, 2005). The A-type granitoid melts were more than 10 % richer in fluorine than the I- or S-type melts. The higher F content in the A-types and specialized S-types could be connected with known metallogenic capacity of these granitoids.

Table 3 represents the results of all calculated values. The halogen equations (Piccoli & Candela, 1994) can also be used to calculate chlorine concentrations, but because most of the studied samples did not contain any chlorine (beyond the detection limit of the microprobe), only the fluorine amounts were calculated.

Table 3: Estimated fluorine content in the granitoid melt and volatile phases after the model of Piccoli & Candela (1994). The fluorine content is in ppm.  $X_{FAP}^{Ap}$  represents the mole fraction of fluorine in apatite,  $X_{HAP}^{Ap}$  represents the mole fraction of hydrogen in apatite,  $C_F^{vol}$  represents the concentration of fluorine in the volatile phase and  $C_F^l$  represents the concentration of fluorine in the melt. Results are statistically evaluated by the average of all the individual values obtained.

	I-type	S-type	A-type	spec.S-type
Number of analyses	34	25	20	28
$X_{FAP}^{Ap}$	0.64	0.63	0.86	0.67
$X_{HAP}^{Ap}$	0.35	0.36	0.14	0.33
$C_F^{aq}$	16	9	229	27
$C_F^l$	88	61	979	296

### Concluding remarks

Apatite distribution and internal structure is different within I-, S- and A-type granitoids. This accessory mineral is abundant in the early magmatic granitoids of the I-type suites and often shows strong zonality because of its long-term crystallization, which occurred deeper than that of S-type granitoids. In contrast, absence of internal structure (uniform grains) is most common in S-type granitoids. Apatites from the Western Carpathians granitoids are present in two colours: milky or white with yellow tones (depending on the Fe content), and dark pigmented (dusky). The latter is more typical for S-type granitoids, but it can be present also in smaller amounts in the I-type granitoids. The compositional impurities in apatite are not as significant compared with structural

peculiarities that need further detailed investigation. Old rounded cores due to inherited material from partial melting are more common in the S-type granitoids.

The composition of apatite grains can be used as a discrimination factor for the division of granitoids into geotectonic suites. Mn and Fe content are the most important discriminative factors. Low Mn content is typical in I-type granitoids, higher Mn and Fe contents are typical of apatites from the S-type granitoids, and the highest Fe content is characteristic of the A-type granitoids.

The amount of fluorine in the melt and in the volatile phase, as calculated from apatite compositions, suggests that S-type granitoids show similar fluorine concentrations in the melt and the volatile phase to I-type granitoids. The highest fluorine content was calculated in the specialized S-type and A-type granitoids, which are of metallogenic significance (e.g. tin-bearing granites in Hnilec area). However, calculations of fluorine contents carry many error factors and they should be taken as a preliminary estimation of initial fluorine content.

### Acknowledgements

The authors are grateful to Julia Kotulová for the carbon investigation in apatite specimen from the Tribeč Mts., as well as to Ivan Dianiška and Pavol Malachovský for providing the samples DD-3 from Dlhá dolina valley borehole. The work was financed by VEGA Ga 4097.

### References

- Broska, I., Dikov, Y.P., Čelková, A. & Mokhov, A.V. 1992: Dusky apatite from the Variscan granitoids of the Western Carpathians. *Geologica Carpathica*, 43, 195-198.
- Broska I., Uher P. 2001: Whole-rock chemistry and genetic typology of the West-Carpathian Variscan granites. *Geol. Carpath.* 52, 2, 79-90.
- Broska I., Kubiš M., Williams C.T. & Konečný P. 2002: The composition of rock-forming and accessory minerals from the Gemeric granites (Hnilec area, Gemeric superunit, Western Carpathians). *Bull. Czech Geol. Survey*, 7, 147-155.
- Broska I., Williams C.T., Uher P., Konečný P. & Leichmann J., 2004: The geochemistry of phosphorus in different granite suites of the Western Carpathians, Slovakia: the role of apatite and P-bearing feldspar. *Chemical geology*, 205, 1-15.
- Cherniak D.J., 2000: Rare earth element diffusion in apatite. *Geochim. et cosmochim. acta* 64, 3871-3885.
- Chovan M. & Határ 1978: Akcesorické minerály niektorých typov hornín kryštalinika veporíd. *Min. Slov.* 10, 9, 24-32.
- Danišík, M., Dunkl, I., Putiš M., Frisch W., Král, M., 2004: Tertiary burial and exhumation history of basement highs along the NW margin of the Pannonian basin – an apatite fission track study. *Austrian J. Earth Sci.*, 95/96, 60-70.
- Dempster, T.J., Jolivet, M., Tubrett, M.N., & Braithwaite, C.J.R. 2003. Magmatic zoning in apatite: a monitor of porosity and permeability change in granites. *Contributions to Mineralogy and Petrology*, 145, 568-577.
- Fleet, M.E., Liu, X. & Pan, Y. 2000: Rare-earth elements in chlorapatite  $[Ca_{10}(PO_4)_6Cl_2]$ : Uptake, site preference, and degradation of monoclinic structure. *American Mineralogist*, 85, 1437-1446.
- Gottesmann, B. & Wirth, R. 1997: Pyrrhotite inclusions in dark pigmented apatite from granitic rocks. *European Journal of Mineralogy*, 9, 491-500.
- Harrison, T.M. & Watson, E.B. 1984: The behaviour of apatite during crystal anatexis: Equilibrium and kinetic considerations. *Geochimica et Cosmochimica Acta*, 48, 1467-1477.
- Hovorka D. & Hvožd'ara P. 1965: Accessory minerals Veporic granitoid rocks I. *Acta geol. Geogr. Univ. Comen. Geol.* 9, Bratislava, 145-179 (In Slovak).

- Hovorka D., 1968: Akcesorické minerály niektorých typov granitoidov Malej Magury, Malej Fatry a Tribča. *Acta geol. et geograph. Univ. Com.* 13, 165-189.
- Hvožd'ara P. & Határ J. 1978: Accessory mineral of some magmatic and metamorphic rocks of veporides. *Acta geol. Geogr. Univ. Comen., Bratislava*, 33, 113-128.
- Král' J. 1977: Fission track ages of apatites from some granitoid rocks in West Carpathians. *Geol. Zbor. Geol. Carpath. Bratislava*, 28, 2, 269-276.
- Kohút, M. 1998: The geochemical and isotopic characteristic of the Hercynian granitoid rocks of the Western Carpathians-Slovakia; evidences for crustal recycling. *Acta Universitatis Carolinae. Geologica*, 42, 276.
- Kubiš M. & Broska I. 2005: Role of Boron and fluorine in evolved granitic rock systems (on an example of the Hnilec area, Western Carpathians). *Geol. Carpath.* 53, 3, 193-204.
- London, D., 1992. Phosphorus in S-type magmas: the  $P_2O_5$  content of feldspars from peraluminous granites, pegmatites and rhyolites. *Am. Mineral.* 77, 126-145.
- London, D., 1998. Phosphorus-rich peraluminous granites. *Acta Univ. Carol. Geol.* 42, 64-68.
- Macek, J., Cambel, B., Kamenicky, L. & Petrík, I. 1982: Documentation and basic characteristics of granitoid rock samples of the West Carpathians. *Geologica Carpathica*, 33, 601-621.
- Marshall, D.J. 1988: Cathodoluminescence of geologic materials. Boston, Unwin Hyman, 146 pp.
- Mathez, E.A. & Webster, J.D. 2005. Partitioning behaviour of chlorine and fluorine in the system apatite-silicate melt-fluid. *Geochimica et Cosmochimica Acta*, 69, 1275-1286.
- Murray, J. R. & Oreskes, N. 1997: Uses and limitations of cathodoluminescence in the study of apatite paragenesis. *Economic Geology*, 92, 368-376.
- Petrík, I., Broska I., & Uher P., 1994: Evolution of the Western Carpathian granite magmatism: Age, source rock, geotectonic setting and relation to the Variscan structure. *Geologica Carpathica*, 45, 283-291.
- Petrík, I. & Broska, I. 1994: Petrology of two granite types from the Tribeč Mountains, Western Carpathians: an example of allanite (+ magnetite) versus monazite dichotomy. *Geological Journal*, 29, 59-78.
- Petrík, I. & Kohút, M. 1997: The evolution of granitoid magmatism during the Hercynian Orogen in the Western Carpathians. In Gre-cula et al. (Eds). : Geological evolution of the Western Carpathians, Bratislava, 235-252.
- Petrík, I. 2000: Multiple sources of the West-Carpathian Variscan granitoids: a review of Rb/Sr and Sm/Nd data. *Geologica Carpathica*, 51, 145-158.
- Piccoli, P. & Candela, P. 1994: Apatite in felsic rocks: a model for the estimation of initial halogen concentrations in the Bishop Tuff (Long Valley) and Tuolumne Intrusive Suite (Sierra Nevada Batholith) magmas. *American Journal of Science*, 294, 92-135.
- Sallet, R. 2000. Fluorine as a tool in the petrogenesis of quartz-bearing magmatic associations: applications of an improved F-OH biotite-apatite thermometer grid. *Lithos*, 50, 241-253.
- Sha, L.-K. & Chappell, B.W. 1999: Apatite chemical composition, determined by electron microprobe and laser-ablation inductively coupled plasma mass spectrometry, as a probe into granite petrogenesis. *Geochimica et Cosmochimica Acta*, 63, 3861-3881.
- Shore, M. & Fowler, A.D. 1996: Oscillatory zoning in minerals: a common phenomenon. *Canadian Mineralogist*, 34, 1111-1126.
- Uher P. & Broska I., 1996: Post-orogenic Permian rocks in the Western Carpathian-Pannonian area: Geochemistry, mineralogy and evolution. *Geol. Carpath.* 47, 311-321.
- Veselský J & Gbelský J. 1978: The results of accessory minerals studies from granitoids and pegmatites of the Malé Karpaty Mts. *Acta geol. et geograph. Univ. Comen., Geol.* 33 Bratislava, 91-111.